16th World Conference on Earthquake, 16WCEE 2017

Santiago Chile, January 9th to 13th 2017

Paper N° 3897 (Abstract ID)

Registration Code: S-M1463097039

Ultimate Strength Calculation Method of RC Outer Walls Subjected to Load from Out-of-plane

A. Obata[(1)], T. Nishida[(2)]

[(1)] *Assistant Professor, Akita Prefectural University, a_obata@akita-pu.ac.jp*
[(2)] *Professor, Akita Prefectural University, tetsuya_nishida@akita-pu.ac.jp*
…

Abstract

The tsunami by the 2011 Tohoku earthquake caused extensive and severe structural damage in north-eastern Japan. The authors conducted a survey of RC structures which is built in the region in received a large tsunami in the Tohoku earthquake. RC outer wall had been the destruction of the square shape. The destruction of RC walls perforated from the out-of-plane direction by the tsunamis.

In this study, the authors are suggesting the ultimate strength calculation method that will contribute from damage experience of such RC outer wall against tsunami wave design. It is considered that the ultimate strength calculation method of the outer wall subjected the tsunami loads from out-of-plane could be applied to use a bending yield line theory at the all four sides supported plate. Further, in the previous study, there were some researching results for the ultimate strength of an all four sides supported plate subjected the out-of-plane load by Dobashi et al. In these researches experimental studies have been made on the ultimate strength calculation of these floor slabs. In this paper, we compare with experimental results of Dobashi et al using a finite element analysis to confirm the validity of the finite element analysis model.

Keywords: RC wall, loads from out-of-plane, ultimate strength, yield line theory, finite element analysis

1. Introduction

On the March 11, 2011 an earthquake occurred off the Pacific coast of Tohoku. The tsunami caused by the 2011 Tohoku earthquake resulted in severe and extensive structural damage in north-eastern Japan. The authors conducted a survey of RC structures, which were built in the region that experienced the large tsunami caused by the Tohoku earthquake. Fig.1 shows an example of destruction of RC outer wall. The RC outer wall, such as the wall of a port warehouse, had been experienced structural damage in shape of a square. The destroyed RC walls were perforated in the out-of-plane direction by the tsunamis and had collapsed. Therefore, in this study, we propose an ultimate strength calculation method that will contribute towards the reduction of damage experienced by such RC outer walls against tsunami waves.

In this study, we initially organized the previous knowledges about calculation method for the ultimate strength of an all four sides supported plate subjected the load from out-of-plane. It is considered that the ultimate strength calculation method of the outer wall subjected to out-of-plane loads caused by the tsunami can be applied by the bending yield line theory on a plate supported on all four sides. Furthermore, the previous studies by Dobashi et al. [1)-3)], focused on the ultimate strength calculation of these floor slabs. In this paper, we compare the test results of Dobashi et al., using a finite element analysis to confirm the validity of the finite element analysis model.

As a result, the results obtained by the finite element analysis are in relatively good correspondence with the previous test results by Dobashi. However, the ultimate strength calculation results obtained by the bending yield line theory for an all four sides supported square plate subjected to out-of-plane loads, are significantly lower in comparison with the finite element analytical results and the test results of Dobashi et al, and the results are not in agreement. In the RC outer wall subjected to out-of-plane loads by tsunami, secondary compressive axial stress is generated in the plane according to the out-of-plane deformation in the wall. This secondary compressive axial stress is considered to increase the ultimate strength. The secondary compressive axial stress obtained by finite element analysis have been enable the re-calculation of the ultimate strength due to bending yield lines of the all four sides supported square plate.

Fig. 1 – An example photo of destruction of RC outer wall

2. Ultimate strength calculation method of the square plates supported on all four sides using the yield line theory

In this paper, the collapse of the RC outer wall is assumed to be due to out-of-plane bending deformation. The ultimate strength of the outer wall can be calculated by the yield line theory. Sometimes the yield line theory had been used in the case of all-four-sides supported square plates, like as calculating ultimate strength of slabs. Fig.

2 shows the collapse mechanism of the RC outer wall based on the yield line theory. The ultimate bending moment per length of yield line of the RC outer wall is shown in M_{p0}. M_{p0} is given by

$$M_{p0} = 0.9\, a_t \cdot \sigma_t \cdot d \tag{1}$$

where a_t, σ_t, and d denote the cross sectional areas of reinforcements, the yield strength of steel bars, and the distance from the edge of compressive side to the position of the tensile steel bars.

In basis of yield line theory, the ultimate strength of the plates may be found from the yield line patterns using either the principle virtual work. Internal work of all models W_{in} is the sum of the internal work by each yield lines. Therefore, in the case of the four sides supported square plate, W_{in} is shown in equation (2). External work W_{out} is given by Equation (3), using a uniformly distributed load par unit area w. From the equation (2) and (3), uniformly distributed ultimate load par unit area w is obtained by the equation (4).

$$W_{in} = 16 M_{p0} \cdot \delta_0 \tag{2}$$

$$W_{out} = wL^2 \frac{\delta_0}{3} \tag{3}$$

$$w = \frac{48 M_{p0}}{L^2} \tag{4}$$

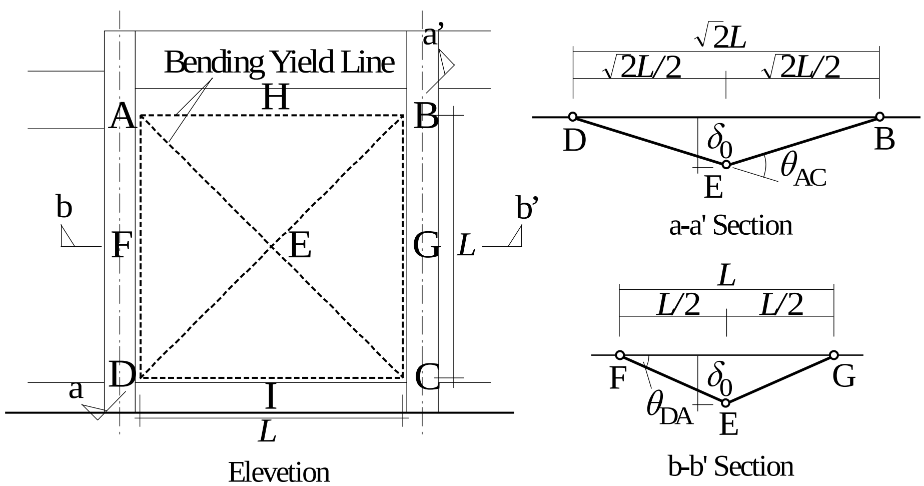

Fig. 2 – Collapse mechanism based on the yield line theory

3. Ultimate strength of the all-four-sides supported square plates obtained by the finite element method

3.1 The ultimate strength test of all-four-sides supported square slabs by Dobashi et al. [1), 2)]

In the previous studies, the ultimate strength test of all-four-sides supported square slabs was performed by Dobashi et al. [1), 2)] The porpose of this test was to clarefy the correspondence between the analytical ultimate strength and the experimental ultimate strength for slubs. Fig. 3 shows an example of the test setup by Dobashi. In this test, the specimens of the square slabs were subjected the 9 pointed loads from out-of-plane by hydraulic jacks.

Some previous studies[4)-6)] had been pointing out that the ultimate strength of the all-four-sides supported square slabs, subjected the load from out-of-plane, had been increased many times by secondary compressive axial stress according to the out-of-plane deformation. Dobashi was also referring to those of previous studies as Johansen's method[5)], modified Park method[6)].

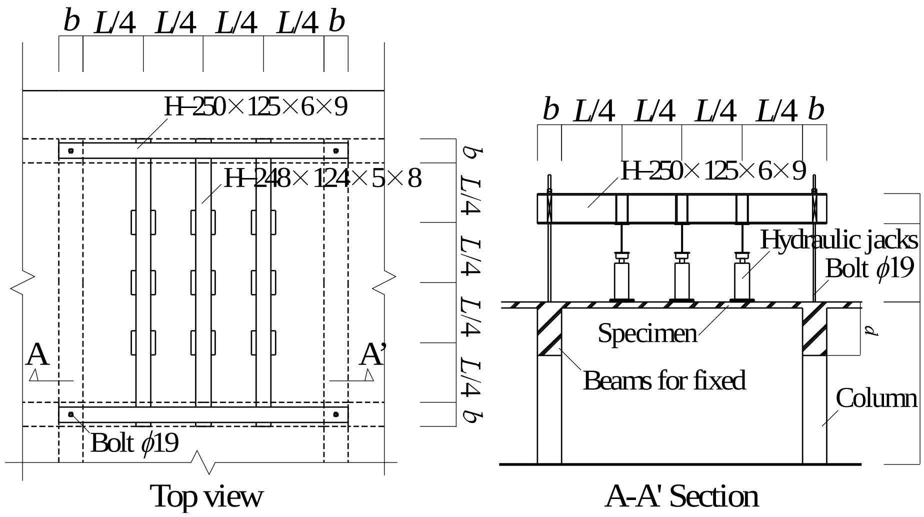

Fig. 3 – An example of test setup by Dobashi et al.[1), 2)]

3.2 Outline of the finite element models

Table 1 shows the details of the finite element models. The analysis models were modeling two kinds of specimens that a single reinforcement was arranged in the center of thickness by Dobashi. The two models size and pitch of the reinforcing bars are equal. Model B has a smaller square plate area and less steel bars number than model A. Further the model B has larger cross section of supported beams than model A. Model B is considered to be relatively higher effect of restraining than model A. Table 2 shows material properties of models referenced to test by Dobashi.

Fig. 4 shows outline of the finite element models. Analysis models are axisymmetric, a quarter of a square plate and supported beams (corresponding to EGBH in Fig. 1). The part of square plate has been modeled by hexahedral 8-node concrete elements, and the steel bars have been modeled by truss elements arranged at the pitch *s*. The models at the parts of square plate thickness direction was divided into two elements. The concrete elements modeling the square plates and truss elements modeling the steel bars have been shared each node. The parts of the supported beams are modeling as a elastic, in order to reproduce in-plane compressive axial force, and the Young's modulus for the beams are equal to the concrete material properties from the test by Dobashi.

The material properties of the finite element models are applying to material characteristic values in test by Dobashi, shown in Table 2. In the material properties of the concrete, the compressive failure envelope is assumed to be multi-liner up to the peak by calcurated from compressive strength F_c and Young's modulus E_c as the Table 2, compressive peak strain 0.2%, forrowed by linear softening. In tension, the tensile strength ${}_c\sigma_t$ is adopted. The material properties of steel bers are assumed to be bi-linear expressed as the yeild stress σ_t and Young's modulus E_s as shown in Table 2.

Loading of finite element models are subjected as shown in Fig 4. There are four pointed loads at the quarters point of horizontal and vertical length on the plate, because of reproducing the 9-point loading test by Dobashi. In Fig. 4, point load *P* represents one point loading value. Total load of this plate is 9*P*. These point loads *P* are increased depending on the loading steps. Diformation angle is calculated from dividing the z-direction displacement of a square plate center point E in the side length of the plate *L*.

Table 1 – Details of the finite element models

model	$L/2 \times L/2$ (mm×mm)	t (mm)	$b \times d$ (mm×mm)
A	1000×1000	52.2	300×750
B	600×600	41.4	450×900

Table 2 – Material properties of the finite element models referenced to the test by Dobashi[1), 2)]

model	Concrete			Steel bar		
	Compressive strength F_c (N/mm^2)	Tensile strength ${}_c\sigma_t$ (N/mm^2)	Young's modulus E_c (N/mm^2)	Cross section	Yield Strength σ_t (N/mm^2)	Young's modulus E_t (N/mm^2)
A	33.1	3.3	2.37×10^4	4ϕ @100	519.4	2.05×10^5
B	22.5	2.2	2.17×10^4		548.8	

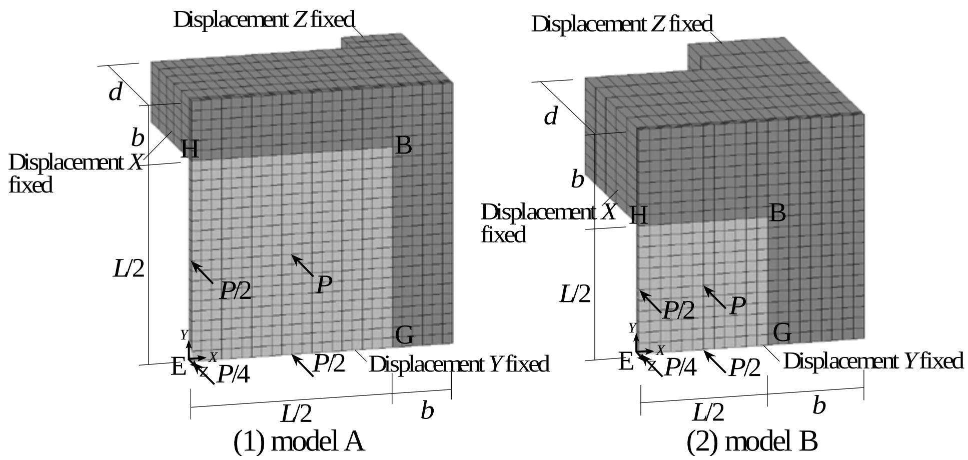

Fig. 4 – Finite element models

3.3 Results of the finite element analysis

Fig. 5 shows the finite element analysis results as the curves of the total loads 9P par unit area versus the deformation angle. Fig. 5 also shows the results of test by Dobashi et al. In Fig. 5, the thickness dashed line shows the ultimate strength calculation results due to bending the yield line theory which were calculated besed on the collapse mechanism shown in Fig. 2. However, in this paper, the loading condition of finite element analysis is the 9-point loading to reproduce the test by Dobashi. Therefore, in this case, the external work ${}_PW_{out}$ and the ultimate strength of 9-point loading P_u is given by follows,

$$ {}_PW_{out} = 5P_u \cdot \delta_0 \tag{5}$$

$$ P_u = \frac{16}{5} M_{p0} \tag{6}$$

In Fig. 5, The finite element analysis results is shown that the displacement is increasing at the small load. It is because the first cracking in the plate was occered. And others, the finite element analysis results is roughly close value compared with results of test by Dobashi.

The values near the downward triangle have indicated the strength values obtained by the test by Dobashi and the strength values obtained by finite element analysis. In this study, the strength obtained by finite element analysis have been adopted the load value of the nearest incremental step of deformation angle in the test of Dobashi. However, in the model B, the strength obtained by finite elemet analysis is employed the load increment step slightly deformed angle is small. It is because that the displacement increment have occured snap-through behaviour on next load step.

The strength obtained by finite element analysis is shown the 87% compared to the strength by Dobashi's test in the model A, and 92% in the model B. The difference of about 10% occurs. On the other hand, the results of the ultimate strength by the yield line theory significantly lower than both finite element results and Dobashi's test results. It is a safety side, but it can not be said a good correspondence. It is from the reason why the RC square plates subjected to the out-of-plane load arise to the secondary compressed axial stress according to out-of-plane deformation. Consequently, it is increase the ultimate strength of the square plate subjected out-of-plane load.

Fig. 6 shows the crack patterns obtained by finite element analytical results. The cracking positions are consistent with the assumed yield line in Fig. 2. This results have indicated that the collapse mechanisms of finite element analysis and the yield line theory are the same. As a results, the assumptions of the yield line in Fig.2 have been correct.

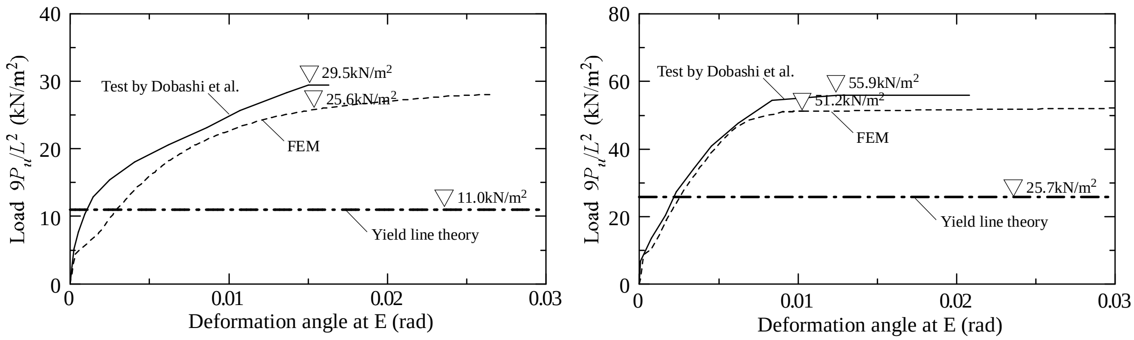

(1) model A (2) model B

Fig. 5 – Load-Deformation curves obtained by FEM analytical results

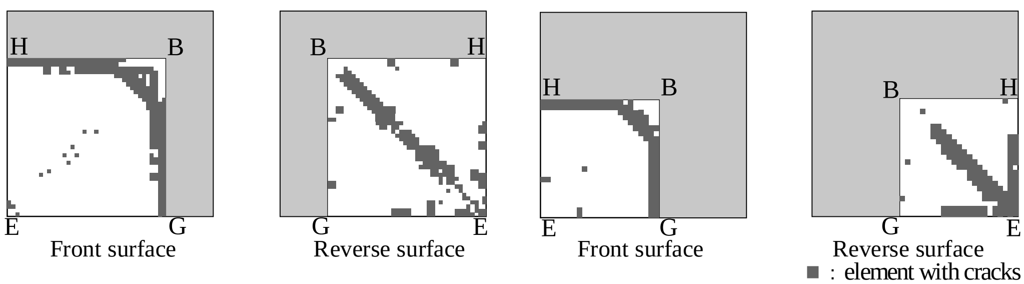

(1) model A (2) model B

Fig. 6 – Crack patterns obtained by FEM analytical results

4. Secondary compressive axial stress of the square plate in-plane supported on all four sides

4.1 Results of the secondary compressive axial stress of the square plate in-plane on the yield line obtained by the finite element analysis

From the finite element analysis results in the model A and model B, the secondary compressive axial stress of square plate in-plane is calculated. At the loading step at the strength obtained by finite element analysis, the axial stress of the nodes on the plate edge GB and the plate diagonal EB as the yield lines in the model A and model B is shown in Fig. 7. In the Fig. 7, the horizontal axis is the y coordinates of the nodes on the square plate edge GB and the square plate diagonal EB, and the vertical axis is the axial stress ratio N/N_0. Where N denote the axial stress at the section and N_0 denote the compressive strength per width at the section of effective area.

In the finite element models, there are some nodes at the same x and y coordinate in the square plate section. Therefore calculation method for the axial stress N considering effective area of each node is required. Axial stress ratio N/N_0 is expressed by the following equation.

$$N/N_0 = \frac{\sum d_{fi} \cdot {}_c\sigma_{xi}}{t \cdot F_c} \tag{7}$$

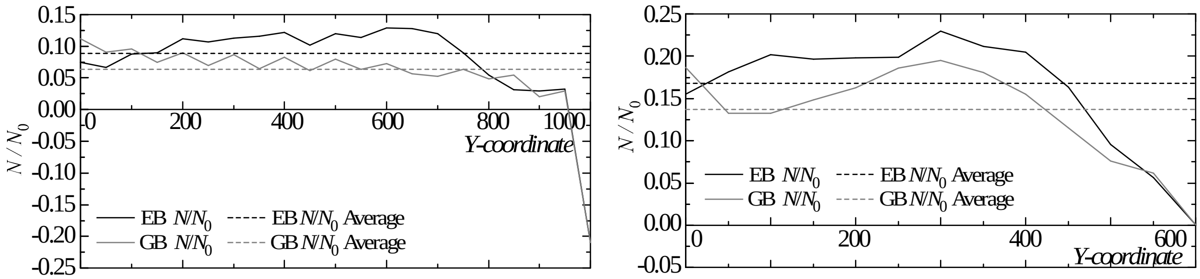

(1) model A (2) model B

Fig. 7 – Axial stress of the nodes on the plate edge GB and the plate diagonal EB

Although Fig. 7 shows the results of the only x-direction stress of the square plate edge GB and square plate diagonal EB, from the reason why the symmetry of the models. The y-direction stress of the square plate edge HB and square plate diagonal EB required the same results of Fig. 7.

In the Fig. 7, the axial stress ratio N/N_0 on the square plate edge GB at the node where steel bar is located shows the stress intensity is lower than the other node. It is greatly affected by the steel bar arrangements. On the other hand, the diagonal EBs nodes are shown less about this effect. The values of the axial stress ratio N/N_0 in the point B are minus of each models corresponding to the corner portions of the four sides supported plates. Near the point B, each model has quite complex stress under the influence of supported by the beams. Also from Crack patterns in Fig. 6, the position near the point B has no cracks and that cracks forming to take chamfer of the corner has been extended.

The average of the axial stress ratios in each yield line, 0.06 at the plate edge GB of model A, 0.09 at diagonal EB of the model A, 0.14 at the plate edge GB of model B, and 0.17 at the diagonal EB of the model B.

4.2 The calculation of the ultimate strength by the yield line theory to consider secondary compressive axial stress in-plane

In the previous section, the secondary compressive axial stress of the square plate in-plane on the yield line obtained by the finite element analysis was clarified. In this section, the authors suggest that the calculation method of the ultimate strength by the yield line theory is modified to consideration of secondary compressive axial stress in-plane.

The ultimate bending moment M_{p0} per length of yield line of the square plate in equation (1) is modified to add the term about the secondary axial stress. The modified ultimate bending moment is shown in equation (8). In equation (8), ${}_cM_{p0}$ denote the ultimate bending moment per length of yield line to consider the effect of secondary axial stress.

$$ {}_cM_{p0} = 0.9\, a_t \cdot \sigma_t \cdot d/s + \frac{N/N_0 \cdot t^2 \cdot F_c}{2}(1 - N/N_0) \tag{8} $$

In addition, Fig 8 shows the relationships between the axial stress ratio N/N_0 versus the ultimate bending moment ${}_cM_{p0}$ in model A and B. In this paper, the value of the average axial stress ratio N/N_0 determined in Section 4.1 is used for simplicity.

Fig. 9 shows the calculation results of the ultimate strength by the yield line theory in consideration of the secondary compressive axial stress. The ultimate strength by the yield line theory in consideration of the secondary compressive axial stress is increased about 3 times to compare with the ultimate strength that is not considering secondary axial stress. And it is close value compared with results of the FEM and test by Dobashi in model A. However, in model B, it is overestimated.

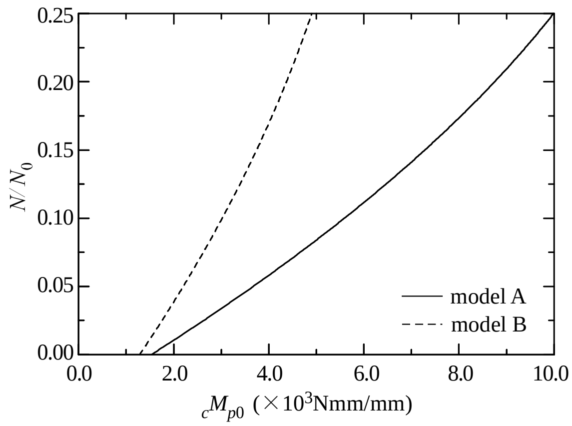

Fig. 8 – Relationships between the axial stress ratio N/N_0 versus the ultimate bending moment $_cM_{p0}$

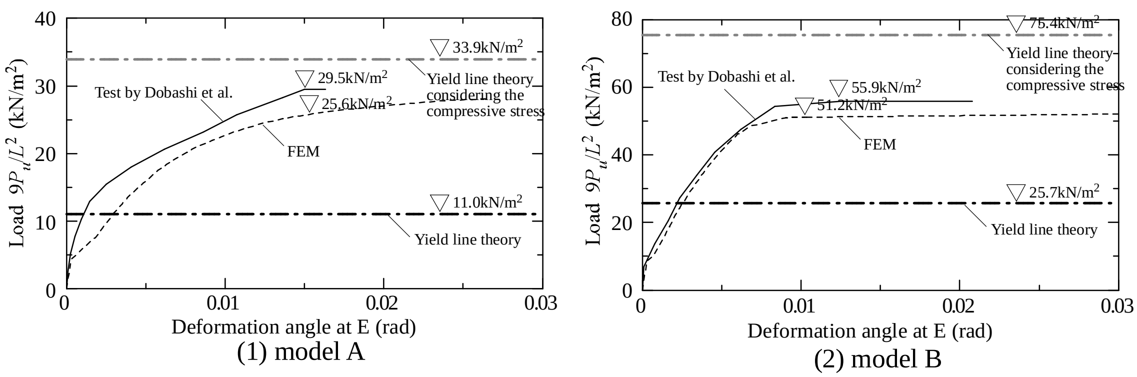

Fig. 9 – Results of the ultimate strength by the yield line theory in consideration of the secondary compressive axial stress.

5. Conclusion

The purpose of this paper is to propose the calculating method about the ultimate strength of RC wall subjectdc to the tsunami load, in response to the collapse of RC outer wall by the tsunami damage caused by the 2011 Tohoku earthquake. Therefore, the authors initially organized the knowledge about calculation for the ultimate strength of an all four sides supported plate subjected the load from out-of-plane. It is considered that the ultimate strength calculation method of the outer wall subjected to loads caused by the tsunami from out-of-plane can be applied by using the bending yield line theory on a plate supported on all four sides. Furthermore, the previous studies by Dobashi et al. 1) - 3), focused on ultimate strength calculation of these floor slabs. So we create a finite element analysis model, we were compared with the results of the ultimate strength calculation method in the yield line theory.

In this paper, the strength obtained by finite element analysis is shown the 87% ~ 92% compared to the strength by Dobashi's test. On the other hand, the results of the ultimate strength by the yield line theory significantly lower than both finite element results and Dobashi's test results. It is safety side, but it can not be said a good correspondence. The cause is that supposed square plate subjected to the out-of-plane load arise to the secondary compressed axial stress according to out-of-plane deformation. Consequently, it is increase the ultimate strength of the square plate subjected out-of-plane load.

Additionally, in this paper, the secondary compressive axial stress obtained by finite element analysis have been enable the re-calculation of the ultimate strength due to bending yield lines of the all four sides supported square plate. As the result, the ultimate strength by the yield line theory in consideration of the secondary compressive axial stress is increased about 3 times to compare with the strength that is not considering secondary axial stress. And it is close value compared with results of the finite element analysis and test by Dobashi in model A. However, in model B, it is overestimated.

References

[1] Yoshizo Dobashi, Kohya Sakajiri (1979): Ultimate Strength of Reinforced Concrete Floor Slabs. *Transactions of Architectural Institute of Japan*, **277**, 1-11.

[2] Kohya Sakajiri, Masahiro Hino, Yoshizo Dobashi (1989): Ultimate Strength of All-edge Built-in Square Floor Slabs of Reinforced Concrete. *Journal of Structural and Construction Engineering*, **403**, 57-65.

[3] Yoshizo Dobashi, Masaiki Ueda (1980): Compressive Membrane Actions In Edge-Restrained Reinforced Concrete Slabs: Comparison of experiments with material-nonlinear solutions with stress reduction due to concrete crushing considered. *Transactions of Architectural Institute of Japan*, **296**, 67-76.

[4] A.J.Ockleston (1958): Arching action in reinforced concrete Slabs. The Structural Engineer, Vol. 36, No. 1.

[5] Johansen, K. W. (1962): Yield-line theory, London, Cement and Concrete Association.

[6] R. Park, W. L. Gamble: Reinforced Concrete Slabs, A wiley-interscience publication.